EBioMedicine 14 (2016) 131–138

Contents lists available at ScienceDirect

EBioMedicine

journal homepage: www.ebiomedicine.com

Research Paper

# Metabolomics Predicts Neuroimaging Characteristics of Transient Ischemic Attack Patients☆

Francisco Purroy, MD, PhD [a,*], Serafi Cambray, PhD [a,1], Gerard Mauri-Capdevila, MD [a,1], Mariona Jové, PhD [b,1], Jordi Sanahuja, MD [a], Joan Farré [c], Ikram Benabdelhak [a], Jessica Molina-Seguin [a], Laura Colàs-Campàs [a], Robert Begue [a], M. Isabel Gil [a], Reinald Pamplona, MD, PhD [b], Manuel Portero-Otín, MD, PhD [b,**]

[a] Stroke Unit, Department of Neurology, Universitat de Lleida, Hospital Universitari Arnau de Vilanova de Leida, Clinical Neurosciences Group IRBLleida, Spain
[b] NUTREN-Nutrigenomics Center, Department of Experimental Medicine, Parc Científic i Tecnològic Agroalimentari de Lleida-Universitat de Lleida-IRBLLEIDA, Lleida, Spain
[c] Laboratori Clinic, Universitari Arnau de Vilanova de Lleida, Clinical Neurosciences Group IRBLleida, Spain

ARTICLE INFO

*Article history:*
Received 2 August 2016
Received in revised form 6 November 2016
Accepted 7 November 2016
Available online 9 November 2016

*Keywords:*
Diffusion magnetic resonance imaging
Metabolomics
TIA

ABSTRACT

*Background:* Neuroimaging is essential for the diagnosis and prognosis of transient ischemic attack (TIA). The discovery of a plasmatic biomarker related to neuroimaging findings is of enormous interest because, despite its relevance, magnetic resonance diffusion weighted imaging (DWI) is not always available in all hospitals that attend to TIA patients.
*Methods:* Metabolomic analyses were performed by liquid chromatography coupled to mass spectrometry in order to establish the metabolomic patterns of positive DWI, DWI patterns and acute ischemic lesion volumes. We used these methods with an initial TIA cohort of 129 patients and validated them with a 2nd independent cohort of 152 patients.
*Findings:* Positive DWI was observed in 115 (40.9%) subjects and scattered pearls in one arterial territory was the most frequent lesion pattern (35.7%). The median acute ischemic lesion volume was 0.33 (0.15–1.90) $cm^3$. We detected a specific metabolomic profile common to both cohorts for positive DWI (11 molecules including creatinine, threoninyl-threonine, *N*-acetyl-glucosamine, lyso phosphatidic acid and cholesterol-related molecules) and ischemic lesion volume (10 molecules including lysophosphatidylcholine, hypoxanthine/threonate, and leucines). Moreover lysophospholipids and creatinine clearly differed the subcortical DWI pattern from other patterns.
*Interpretation:* There are specific metabolomic profiles associated with representative neuroimaging features in TIA patients. Our findings could allow the development of serum biomarkers related to acute ischemic lesions and specific acute ischemic patterns.
© 2016 The Authors. Published by Elsevier B.V. This is an open access article under the CC BY-NC-ND license (http://creativecommons.org/licenses/by-nc-nd/4.0/).

## 1. Introduction

Magnetic resonance diffusion weighted imaging (DWI) remains the best neuroimaging technique to detect acute ischemia, above all since the new tissular definition of transient ischemic attack (TIA) has become essential in the evaluation of TIA patients (Easton et al., 2009). According to a recent meta-analysis, despite transient clinical symptoms, one out of three patients with definite TIA has an acute DWI lesion (Brazzelli et al., 2014). Moreover, DWI has been shown to be an important predictor of early stroke recurrence (Purroy et al., 2004) and it has been proposed to add to clinical prognostic scales like ABCD2I (Giles et al., 2011) and ABCD3I (Merwick et al., 2010). Furthermore, not only the presence but also the patterns of DWI are important both for the etiological classification and for patient prognosis (Purroy et al., 2011). However, despite the increased availability of magnetic resonance imaging (MRI) not all TIA patients undergo DWI. Therefore, the discovery of a plasmatic biomarker related to neuroimaging findings is of enormous interest.

The use of metabolomics on TIA patients has started a new era in biomarker discovering for clinical purpose (Jove et al., 2015a). Metabolomics allows the study of the complete set of low-molecular-weight intermediates (metabolites), which vary according to the pathologic state of the cell, tissue, organ, or organism and are context-dependent (Jove et al., 2014; Mauri-Capdevila et al., 2013).

☆ Authors report non-disclosures.
* Correspondence to: F. Purroy, Stroke Unit, Department of Neurology, Universitat de Lleida, Hospital Universitari Arnau de Vilanova de Lleida, Clinical Neurosciences Group IRBLleida, Avda Rovira Roure, 80, Lleida 25198, Spain.
** Corresponding author.
*E-mail address:* fpurroygarcia@gmail.com (F. Purroy).
[1] These authors contributed equally to this work.

http://dx.doi.org/10.1016/j.ebiom.2016.11.010
2352-3964/© 2016 The Authors. Published by Elsevier B.V. This is an open access article under the CC BY-NC-ND license (http://creativecommons.org/licenses/by-nc-nd/4.0/).

The aim of the present study was to perform a metabolomic analysis to find new biomarkers associated with the presence of acute DWI lesion and the volume and patterns of these lesions. As previously (Jove et al., 2015a), results were validated in an independent cohort.

## 2. Methods

### 2.1. Subjects

This study was approved by the ethics committee of the Arnau de Vilanova University Hospital. The main methodology has been previously described (Jove et al., 2015a). We prospectively recruited two independent cohorts of consecutive TIA patients who were attended to by a neurologist during the first 24 h after the onset of symptoms. Both cohorts shared the same methodology but were recruited at different times (Fig. 1). We excluded 12 patients with contraindications to MRI from the original study. We therefore analyzed 129 patients from cohort 1 and 152 patients from cohort 2. TIA was defined according to the classical definition as acute onset of focal cerebral or monocular symptoms lasting <24 h and thought to be attributable to a brain ischemia (Anon, 1990). In order to avoid ethnic differences in the observed metabolomic profiles, all the patients included were Caucasian in origin. Patients were classified etiologically according to the Trial of ORG 10172 (TOAST) (Adams et al., 1993). Undetermined territory included patients without higher brain function disturbance such us aphasia, hemianopsia, neglect, or vertebrobasilar symptoms. Vertebrobasilar TIA was characterized by the following symptoms: bilateral or shifting motor or sensory dysfunction, complete or partial loss of vision in homonymous fields, dizziness, vertigo, or any combination thereof (Purroy et al., 2011).

### 2.2. Neuroimaging Protocol

A MRI was acquired using a 1.5-T whole-body system with a 24-mT/m gradient strength, 300 ms rise time, and an echo-planar–capable receiver equipped with a gradient overdrive (Philips Intera 1.5 T, MRI scanner). The images obtained included axial T2-weighted turbo spin-echo (TR/TE: 4800/120), T1-weighted spin-echo (TR/TE: 540/15), axial turbo fluid-attenuated inversion recovery (TR/TI/TE: 8000/2200/120), and echo-planar diffusion images (TR/TE: 3900/95). The field of view was 230 mm and the matrix was 256 × 256 in all sequences. The DWI were obtained with a single-shot spin-echo echo-planar pulse sequence with diffusion gradient b values of 1000 s/mm2 along orthogonal axes over 20 axial sections, using 6 mm thick sections, and an interslice gap of 1 mm. Tissue abnormality (positive DWI) was defined as areas of high signal intensity on isotropic DWI reflecting an acute ischemic lesion. Patterns of DWI were determined according to a previous definition (Purroy et al., 2011): DWI normality, scattered pearls in one arterial territory (SPOT), multiple vascular territories, a single cortical lesion in one vascular territory and a subcortical pattern. Two Neuroradiologists blinded to clinical features established the presence and patterns of DWI abnormalities. The interobserver agreement (kappa value) is 1.0 for identifying positive DWI and 0.98 for identifying DWI patterns. Furthermore, OsiriX V.4.0 imaging software (Rosset et al., 2004) was used to calculate the total volume of DWI abnormality. We manually outlined the respective abnormalities using the OsiriX closed polygon tool, thereby creating a region of interest (ROI). ROIs in between the segmented slices were interpolated automatically. The resulting DWI abnormality volume was then determined.

### 2.3. Metabolomic Analysis

For non-targeted metabolomic analysis, plasma samples were obtained in the morning in order to avoid diurnal variations and metabolites were extracted with methanol according to previously described methods (Wikoff et al., 2008). Briefly stated, 90 μl of cold methanol (containing phenylalanine-C13 as an internal standard) were added to 30 μl of plasma, incubated for one hour at −20 °C and centrifuged for three minutes at 12,000g. The supernatant was recovered, evaporated

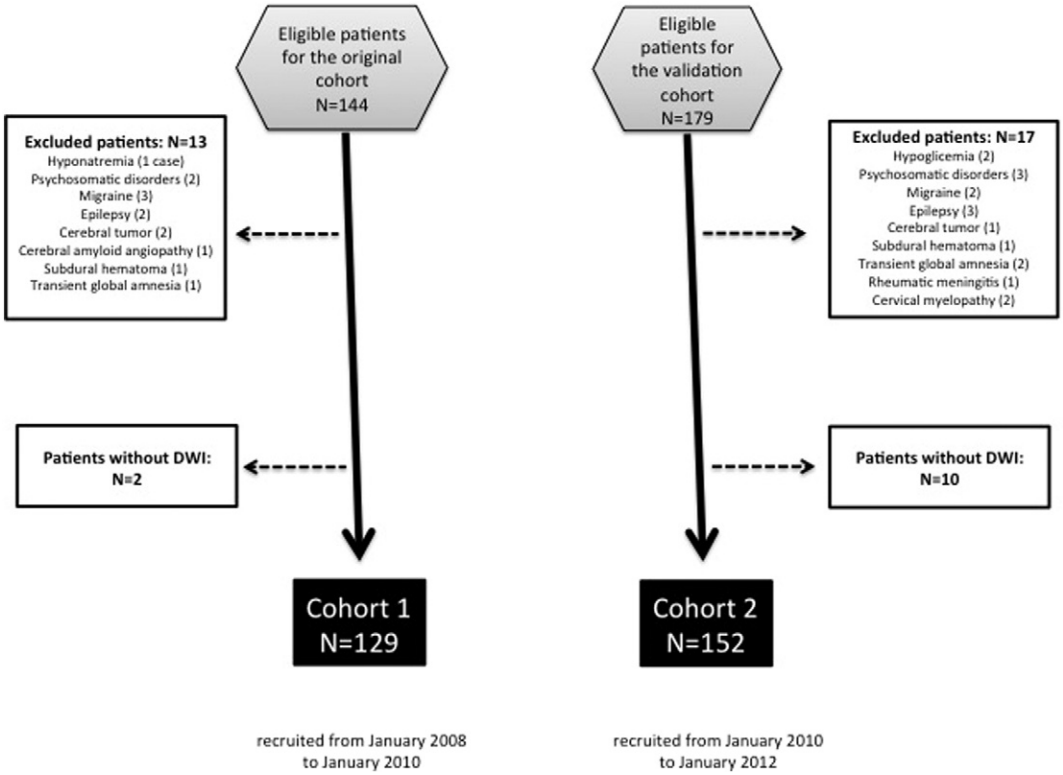


**Fig. 1.** Patient inclusion chart.

using a Speed Vac (Thermo Fisher Scientific, Barcelona, Spain) and resuspended in water containing 0.4% acetic acid/methanol (50/50).

We used an ultra-high pressure liquid chromatography (UHPLC) scheme with an Agilent 1290 LC system coupled to an electrospray-ionization quadruple time of flight mass spectrometer (Q-TOF) 6520 instrument (Agilent Technologies, Barcelona, Spain). A column with a particle size of 1.8 μm was employed. The preliminary identification of differential metabolites was performed using the PCDL database from Agilent (Agilent Technologies, Barcelona, Spain), which uses retention times, exact mass and isotope distribution in an standardized chromatographic system as an orthogonal searchable parameter to complement accurate mass data (AMRT approach) according to previously published works (Sana et al., 2008). The version of the PCDL database used had retention times and accurate mass data for 679 compounds.

### 2.4. Statistical Analysis

Statistics calculations were performed using the SPSS software version 20 (SPSS, Chicago, IL) or the Stata 11 statistics package (StataCorp, College Station, TX). Normal distribution of the variables was checked by the Kolmogorov-Smirnoff test. Partial least discriminate analysis (PLS-DA) was performed using Mass Molecular Profiler software (Agilent Technologies, Barcelona, Spain). Briefly stated, the number of components chosen for PLS-DA was 4, and data were scaled using an auto scaling algorithm. Validation of the model was achieved with a N-fold validation type with 3 folds and 10 repeats as validation parameters. In all cases, significance was considered for $p < 0.05$.

Statistical significance for intergroup differences was assessed using the $X^2$ test for categorical variables and the Student's *t*-test, ANOVA test and Mann-Whitney *U* test for continuous variables. Univariate analyses were performed to detect variables associated with the presence of positive DWI and DWI patterns. Assuming that the ischemia volume determined on DWI could be considered to constitute a continuous variable, we tested whether any circulating metabolite could be correlated with it. Receiver operating characteristic (ROC) curves for metabolomic data were performed using the ROCCET platform. ROC curves were plotted to predict the presence of positive DWI and DWI patterns.

## 3. Results

As we have published previously, we did not find any statistically significant differences between the two cohorts based on vascular risk factors, clinical characteristics and neuroimaging data (Jove et al., 2015b). We observed DWI abnormalities in 115 (40.9%) patients. Moreover, SPOT pattern, present in 41 (35.7%) patients, was the most frequent pattern (Table 1). Clinical features, vascular risk factors and etiology varied significantly among the different DWI patterns (Table 2). Patients who had DWI abnormalities in multiple territories were older than patients with other patterns. Motor weakness was more frequent among subcortical lesion and multiple territories pattern. LAA was the most frequent etiology among SPOT. Moreover, SPOT and multiple territories pattern had higher volumes of DWI lesion. The median acute ischemic lesion volume was 0.33 (0.15–1.90) $cm^3$.

### 3.1. Metabolomics and Positive DWI

Following metabolomic analyses of the discovery and validation cohorts, a distinctive pattern of metabolites was found. As shown in the heatmap (Fig. 2A), positive DWI exhibited a differential metabolomic profile in the discovery cohort. For PLSDA modeling, a three-component model with a high degree of accuracy (0.62, R2 = 0.85) was obtained in the discovery cohort (Fig. 2A). Similarly, the PLSDA model in the validation cohort also reached a high degree of accuracy (0.64, R2 = 0.96, Fig. 2B). In addition to the separation offered by the PLSDA plot, whose axis showed the integration of multiple compounds, we explored the capacity of individual metabolites to explain separation between DWI and non-DWI groups. The results (Fig. S1) revealed that several molecules could differentiate these groups, with receiving operating characteristic curves consistent in both cohorts. Univariate statistics showed that a total of 87 molecular features in the discovery cohort were significantly different between positive DWI and normal DWI patients (Student's *t*-test, p values between 6.98 E−5 and 0.05, supplemental dataset 1). After applying the same approach to the validation cohort, 379 molecular features showed significant differences between these two groups (Student's *t*-test, p values between 2.34 E−5 and 0.05, supplemental dataset 1). When searching for common differential molecular features shared by these two cohorts, 11 molecular features were found (Table 3). When we applied a database search using the PCDL software (integrating exact masses, isotope distribution and retention time identity with an identical LC/MS system) it was possible to propose several identities (Table 3), including creatinine, threoninyl-threonine, *N*-acetylglucosamine, lysophosphatidic acid (LPA) and a cholesterol-related molecule. Most differential compounds showed ROC areas (data not shown) between 0.6 and 0.65, demonstrating that these molecules could serve as potential biomarkers for acute ischemic lesions on DWI.

**Table 1**
Risk factors, clinical characteristics and neuroimaging data of both cohorts.

| Variable | Cohort 1 (n = 129) | Cohort 2 (n = 152) | Total (n = 281) | p |
|---|---|---|---|---|
| Vascular risk factors | | | | |
| Age, mean (SD) | 71.1 (10.4) | 71.8 (11.2) | 71.5 (10.8) | 0.623 |
| Male | 83 (64.3) | 91 (59.9) | 174 (61.9) | 0.442 |
| Previous stroke | 28 (21.7) | 34 (22.5) | 62 (22.1) | 0.894 |
| Hypertension | 89 (69.0) | 102 (67.1) | 191 (68.0) | 0.735 |
| Coronary disease | 17 (13.2) | 20 (13.2) | 37 (13.2) | 0.996 |
| Diabetes mellitus | 40 (31.0) | 44 (28.9) | 84 (29.9) | 0.707 |
| Smoking | 18 (14.0) | 18 (11.8) | 36 (12.8) | 0.598 |
| Hypercholesterolemia | 49 (38.0) | 59 (38.8) | 108 (38.4) | 0.886 |
| Previous atrial fibrillation | 17 (13.2) | 15 (9.9) | 32 (11.4) | 0.384 |
| Basal treatments | | | | |
| Aspirin | 30 (23.3) | 36 (23.8) | 66 (23.6) | 0.908 |
| Clopidogrel | 8 (6.2) | 17 (11.3) | 25 (8.9) | 0.139 |
| Anticoagulation | 19 (14.7) | 10 (6.6) | 29 (10.4) | 0.026 |
| Statins | 43 (33.6) | 46 (30.5) | 89 (31.9) | 0.576 |
| Renin-angiotensin system blockers | 64 (49.6) | 71 (47.7) | 135 (48.6) | 0.744 |
| Clinical features | | | | |
| Duration | | | | |
| < 10′ | 12 (9.3) | 16 (10.5) | 28 (10.0) | 0.925 |
| 10–59′ | 49 (38.0) | 56 (36.8) | 105 (37.4) | |
| 1 h | 68 (52.7) | 80 (52.6) | 148 (52.7) | |
| Cluster TIA | 35 (27.1) | 33 (21.7) | 68 (24.2) | 0.290 |
| Weakness | 69 (53.5) | 78 (51.3) | 147 (52.3) | 0.716 |
| Isolated sensory symptoms | 12 (9.3) | 13 (8.6) | 25 (8.9) | 0.826 |
| Speech impairment | 76 (58.9) | 94 (62.3) | 170 (60.7) | 0.569 |
| Vertebrobasilar | 10 (7.8) | 12 (7.9) | 22 (7.9) | 0.952 |
| ABCD2, median (IQR) | 5.2 (4.0–6.0) | 5.1 (4.0–6.0) | 5.1 (4.0–6.0) | 0.753 |
| Etiological subtypes | | | | |
| Large artery atherosclerosis | 32 (24.8) | 29 (19.2) | 61 (21.8) | 0.509 |
| Cardioembolism | 23 (17.8) | 35 (23.2) | 58 (20.7) | |
| Small-vessel disease | 28 (21.7) | 29 (19.2) | 57 (20.4) | |
| Undetermined cause | 46 (35.7) | 58 (38.4) | 104 (37.1) | |
| Neuroimaging features | | | | |
| DWI abnormality | 59 (45.7) | 56 (36.8) | 115 (40.9) | 0.145 |
| Scattered pearls on one territory | 18 (14.0) | 23 (15.4) | 41 (14.7) | 0.485 |
| Multiple territories | 4 (3.1) | 3 (2.0) | 7 (2.5) | |
| Single cortical lesion | 18 (14.0) | 16 (10.7) | 34 (12.2) | |
| Subcortical lesion | 19 (14.7) | 14 (9.4) | 33 (11.9) | |
| DWI normality | 70 (54.3) | 93 (62.4) | 163 (58.6) | |
| DWI volume, mean (SD) | 0.36 (0.15–1.91) | 0.33 (0.15–2.45) | 0.33 (0.15–1.90) | 0.987 |

Percentages are shown in parentheses as appropriate.
DWI, diffusion-weighted images; TIA, transient ischaemic attacks; SD, standard deviation; IQR, interquartile range.

**Table 2**
Risk factors and clinical features by DWI patterns.

| Variable | All cases (n = 281) | DWI normality (n = 166) | Scattered pearls one territory (n = 41) | Multiple territories (n = 7) | Single cortical lesion (n = 34) | Subcortical lesion (n = 33) | p |
|---|---|---|---|---|---|---|---|
| Vascular risk factors | | | | | | | |
| Age, mean (SD) | 71.5 (10.8) | 73.4 (9.9) | 69.2 (11.3) | 74.1 (5.5) | 68.8 (13.8) | 67.2 (10.2) | 0.005 |
| Male | 174 (61.9) | 95 (57.2) | 32 (78.0) | 5 (71.4) | 20 (58.8) | 22 (66.7) | 0.165 |
| Hypertension | 191 (68.0) | 118 (71.1) | 27 (65.9) | 4 (57.1) | 20 (58.8) | 22 (66.7) | 0.687 |
| Previous stroke | 62 (22.1) | 42 (25.3) | 8 (19.5) | 2 (28.6) | 7 (20.6) | 3 (9.1) | 0.340 |
| Diabetes mellitus | 84 (29.9) | 58 (34.9) | 7 (17.1) | 1 (14.3) | 9 (26.5) | 9 (27.3) | 0.175 |
| Coronary disease | 37 (13.2) | 23 (13.9) | 6 (14.6) | 1 (14.3) | 6 (17.6) | 1 (3.0) | 0.448 |
| Smoking | 36 (12.8) | 13 (7.8) | 8 (19.5) | 0 (0) | 7 (20.6) | 8 (24.2) | 0.020 |
| Hypercholesterolemia | 108 (38.4) | 64 (38.6) | 17 (41.5) | 5 (71.4) | 18 (52.9) | 4 (12.1) | 0.003 |
| Previous atrial fibrillation | 32 (11.4) | 20 (12.3) | 9 (22.0) | 1 (14.3) | 1 (2.9) | 1 (3.0) | 0.054 |
| Clinical features | | | | | | | |
| Cluster TIA | 68 (24.2) | 31 (19.0) | 13 (31.7) | 3 (42.9) | 9 (26.5) | 10 (30.3) | 0.216 |
| Speech impairment | 170 (60.7) | 103 (63.6) | 20(48.8) | 3 (42.9) | 19 (55.9) | 22 (66.7) | 0.317 |
| Motor weakness | 147 (52.3) | 68 (41.0) | 27 (65.9) | 5 (71.4) | 21 (61.8) | 26 (78.8) | <0.001 |
| Isolated sensory symptoms | 25 (8.9) | 20 (12.0) | 1 (2.4) | 1 (14.3) | 0 (0) | 3 (9.1) | 0.096 |
| Vertebrobasilar symptoms | 22 (7.9) | 11 (6.7) | 4 (9.8) | 1 (16.7) | 3 (8.6) | 3 (9.1) | 0.867 |
| Lacunar syndrome | 105 (37.5) | 61 (36.6) | 15 (36.6) | 0 (0) | 9 (25.7) | 20 (62.5) | 0.007 |
| Duration (n = 272) | | | | | | | 0.087 |
| < 10′ | 28 (10.0) | 22 (13.3) | 3 (7.3) | 1 (14.3) | 0 (0) | 2 (6.1) | |
| 10–59′ | 105 (37.4) | 58 (34.9) | 16 (39.0) | 2 (28.6) | 20 (58.8) | 9 (27.3) | |
| 1 h | 148 (52.7) | 86 (51.8) | 22 (53.7) | 4 (57.1) | 14 (41.2) | 22 (66.7) | |
| ABCD2, median (IQR) | 5.1 (4.0–6.0) | | | | | | |
| Etiological subtypes | | | | | | | |
| Large artery disease | 61 (21.8) | 30 (18.1) | 16 (39.0) | 2 (28.6) | 11 (32.4) | 2 (6.1) | <0.001 |
| Cardioembolism | 58 (20.7) | 34 (20.5) | 13 (31.7) | 2 (28.6) | 7 (20.6) | 2 (6.1) | |
| Small vessel disease | 57 (20.4) | 33 (19.9) | 0 (0) | (0) | (0) | 29 (87.9) | |
| Undetermined | 99 (35.2) | 68 (41.0) | 12 (29.3) | 3 (42.9) | 16 (47.1) | 0 (0) | |
| DWI volume, mean (SD) | 0.33 (0.15–1.90) | – | 0.67 (0.28–2.99) | 0.49 (0.04–1.19) | 0.27 (0.07–7.17) | 0.23 (0.17–0.68) | 0.079 |

Percentages are shown in parentheses as appropriate.
DWI, diffusion-weighted images; TIA, transient ischaemic attacks; SD, standard deviation; IQR, interquartile range.

### *3.2. Metabolomics and Acute Ischemic Lesion Volume*

In the discovery cohort, 43 molecules showed a significant correlation with acute ischemic lesion volume (Pearson correlation test, p values between 3.12 E−07 and 0.05, Supplementary dataset 2). In the validation cohort 211 molecules showed this feature (Pearson correlation test, p values between 1.31 E−10 and 0.05, supplementary data set 2). After searching for common molecules, a total of 7 different molecules were found including lysophosphatidylcholine, hypoxanthine/threonate, and leucine (Table 4). Globally, these molecules showed a significant direct relationship with ischemia volume.

### *3.3. Metabolomics and DWI Patterns*

The results for the discovery cohort suggest specific metabolomic profiles that cluster patients according to their DWI pattern. Subcortical pattern patients were therefore clearly different from those with isolated cortical lesions and those with normal DWI according to a PLSDA model with a moderate degree of accuracy (two-component model 0.503, R2 0.63, Fig. 3A). This was confirmed by the analysis in the confirmation cohort, where accuracy increased (two-component model 0.58, R2 0.92, Fig. 3B). This supported the notion that, according to the metabolomic profiles, the subcortical DWI pattern could be clearly differed from other patterns, such us isolated cortical lesions and DWI negative patients. A random forest classification scheme confirmed these findings, with subcortical patterns being classified with lower margin of error (<0.05) in both cohorts.

In the case of univariate measurements, in the first cohort a total of 81 molecules were seen to be significantly different from these patterns (p values ranging between 2E−04 and 0.05, Supplemental dataset 3). In the confirmation cohort, 285 molecules differed across the DWI pattern (p values between 5.94E−11 and 0.05, Supplemental dataset 3). Confirming the existence of potential biomarkers for the DWI pattern, 8 molecules were found to be common between these two cohorts (Table 5). These comprised lysophospholipids, as well as creatinine and other unknown metabolites.

## 4. Discussion

To the best of our knowledge, this is the first time that a metabolomics approach has revealed potential biomarkers related to neuroimaging findings after TIA. Previous data from different groups related metabolomics data with neuroimaging in the context of bipolar disorder (McIntyre et al., 2014), multiple sclerosis (Vingara et al., 2013), dementia such as Alzheimer's disease (Lista et al., 2015), schizophrenia (Waddington, 2007), Parkinson disease (Ren et al., 2015) and even pediatric cerebral infections (Pappa et al., 2015). We found a specific metabolomic profile related to acute ischemic lesions, volume and specific acute ischemic patterns. In a previous report, Bivard et al. (2014), using magnetic resonance spectroscopy, discovered in ischemic stroke patients with posttreatment hyperperfusion signs of increased glutamate, *N*-acetylaspartate and lactate. These changes were related to increased metabolism and potentially enhanced ulterior neuroplasticity. In our case, positive DWI was linked to changes in several other metabolites, such as creatinine, *N*-acetyl-glucosaminylamine and LPA. Interestingly, *N*-acetyl-glucosaminylamine, that is structurally related to *N*-acetyl-glucosamine, and other similar molecules are modulators of immune response (Srikrishna et al., 2001) when expressed at the endothelial membrane. Assuming the important role of microglia and activated neutrophils in brain ischemia response (Amantea et al., 2015), the present findings could be in line with changes in expression and cleavage of glycoprotein components. It should be noted that, one of the potential markers for DWI positivity was a low level of LPA. These molecules, and their signaling through their cognate receptor LPA1, have been implicated in the generation of ischemia-related neuropathic pain (Halder et al., 2013). Moreover, some molecules from this family are also considered angiogenic factors (Ren et al., 2011; Binder et al., 2013). Therefore, diminished levels may be associated with a lower capacity to withstand hypoxia-induced apoptosis (Liu et al., 2009). Interestingly, other

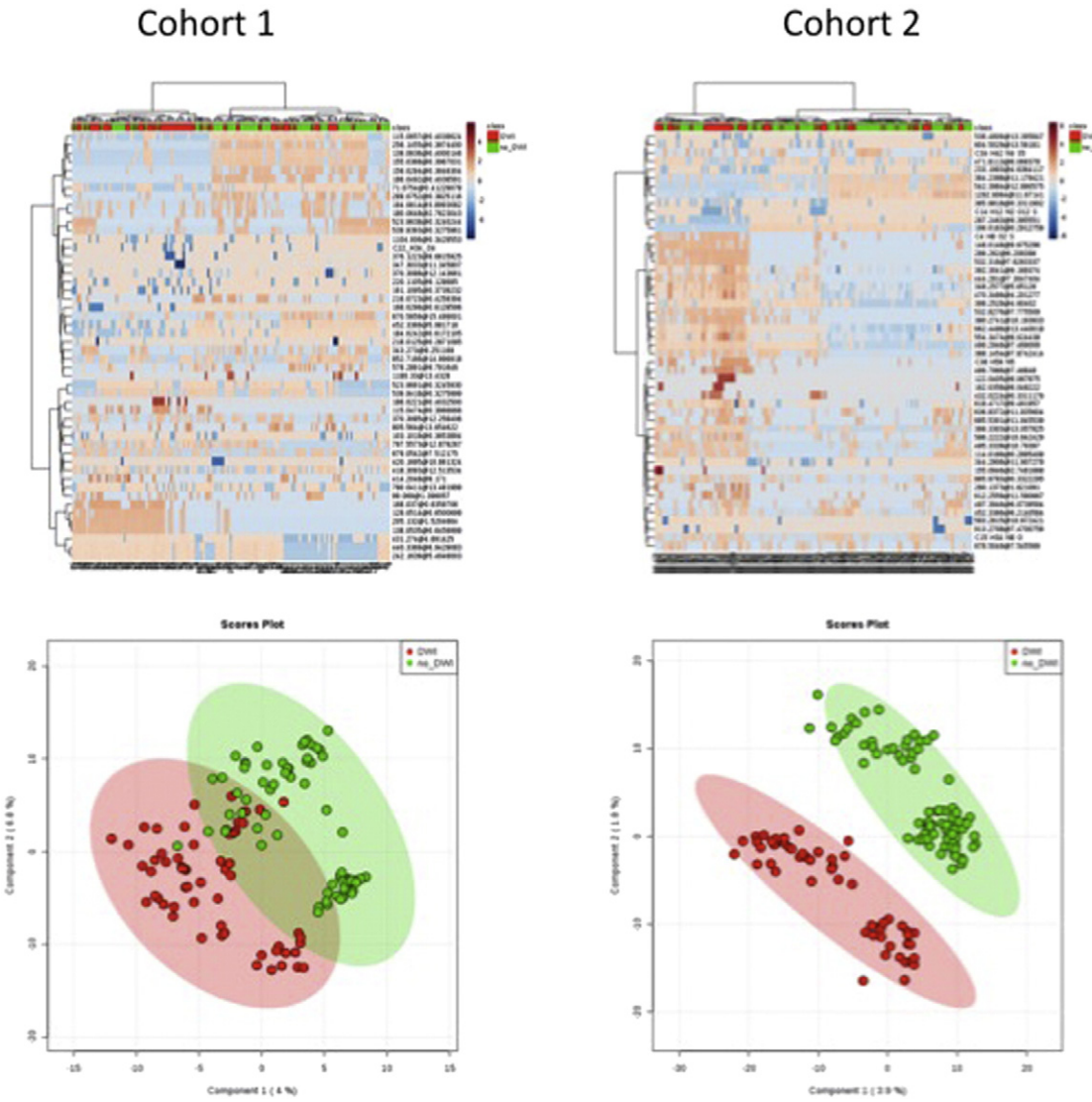


**Fig. 2.** Association of DWI with differential metabolomic patterns. Upper panels: heatmap showing major metabolites differentiating plasma metabolomic profiles from DWI positive versus non DWI positive patients, both in the discovery cohort (A) and in the validation cohort (B). A PLSDA model could be designed with a high accuracy, as shown in the lower panels, both for the discovery cohort (A) and for the validation cohort (B).

researchers have found increased LPA in plasma from patients with vascular cerebral ischemia (Li et al., 2008). In this context, both activated platelets and atheroma plaque are known sources of LPA (Haseruck et al., 2004). The fact that LPA is a platelet activator and thrombotic agent reveals the potential involvement of these molecules in cerebral changes linked to hypoxia. In order to explain whether the decreased LPA observed in our DWI positive patients is a protective trait (in light of its thrombogenic role) or a negative feature (based on the antiapoptotic properties), it should be taken into account that we have specifically found an increase in LPA (O-20:0). Furthermore, the

**Table 3**
Molecular features differing between positive DWI and negative DWI patients.

| Metabolite Identification[a] | Discovery cohort | | | Validation cohort | | |
|---|---|---|---|---|---|---|
| | Mass | RT (min) | p value[b] | Mass | RT (min) | p value[b] |
| LysoPA(O-20:0)/5alpha-cholestane-3alpha,7alpha,12alpha,23,25-pentol | 452.34 | 5.98 | 0.011 | 452.34 | 6.21 | 0.001 |
| Unknown 1 | 218.01 | 0.29 | 0.028 | 218.01 | 0.21 | 0.007 |
| Unknown 2 | 220.11 | 9.13 | 0.006 | 220.11 | 9.13 | 0.008 |
| Creatinine | 113.06 | 0.38 | 0.050 | 113.06 | 0.38 | 0.012 |
| Threoninyl-Threonine/*N*-acetyl-b-glucosaminylamine/DiHDPA | 362.25 | 11.67 | 0.009 | 362.25 | 11.94 | 0.012 |
| Unknown 3 | 216.07 | 0.43 | 0.007 | 216.08 | 0.56 | 0.013 |
| Unknown 4 | 154.97 | 0.14 | 0.023 | 154.97 | 0.28 | 0.013 |
| Unknown 5 | 157.99 | 0.30 | 0.039 | 157.99 | 0.23 | 0.017 |
| Unknown 6 | 146.07 | 0.41 | 0.019 | 146.07 | 0.39 | 0.038 |

RT, retention time; LysoPA, lysophosphatidic acid.
[a] Potential identities, based on retention time and exact mass are presented. When it is not possible to attribute only one identity, two or three potential identities are shown.
[b] After Student's *t*-test between positive DWI and negative DWI patients.

**Table 4**
Molecular features correlating with acute ischemic lesion volume.

| Identification[a] | Discovery cohort | | | | Validation cohort | | | |
|---|---|---|---|---|---|---|---|---|
| | Mass | RT (min) | Pearson correlation coefficient[b] | p value | Mass | RT (min) | Pearson correlation coefficient[b] | p value |
| LysoPC (22:6) | 567.33 | 10.72 | 0.20 | 0.06 | 567.33 | 10.89 | 0.29 | 0.00 |
| Hypoxanthine/threonate | 136.04 | 0.78 | 0.20 | 0.06 | 136.04 | 0.78 | 0.23 | 0.01 |
| Unknown 1 | 294.19 | 9.36 | 0.18 | 0.09 | 294.19 | 9.41 | 0.19 | 0.02 |
| LysoPC (20:4)[c] | 543.33 | 10.68 | 0.18 | 0.08 | 543.33 | 11.10 | 0.18 | 0.03 |
| Unknown 2 | 760.03 | 0.34 | -0.21 | 0.05 | 760.02 | 0.33 | -0.16 | 0.04 |
| Isoleucine/leucine/norleucine | 131.09 | 0.56 | 0.30 | 0.00 | 131.09 | 0.55 | 0.16 | 0.05 |
| Unknown 3 | 85.09 | 0.56 | 0.29 | 0.01 | 85.09 | 0.55 | 0.16 | 0.06 |

RT, retention time; LysoPC, lysophosphatidylcholine.
[a] Potential identities, based on retention time and exact mass are presented. When it is not possible to attribute only one identity, two or three potential identities are shown.
[b] Correlation coefficient with ischemia volume.
[c] Note the difference in RT between the two cohorts. No peak with similar exact mass and isotope distribution was found closer to the first retention time.

structure-function relationships for LPAs are strongly dependent on the side chain (Haseruck et al., 2004).

As in our previous work (Jove et al., 2015b), specific patterns of LysoPC were again relevant. LysoPC (22:6) and LysoPC (20:4), that were previously related to LAA and stroke recurrence respectively, were now associated with lesion volume. Furthermore, LysoPC (16:0), that was low in those TIA patients who suffered a subsequent stroke, was now related to SPOT and cortical patterns. All these associations made sense because SPOT and cortical patterns which are overrepresented in LAA patients (Purroy et al., 2011) had the biggest lesion volume.

Our work shows some inherent limitations. The fact that the patients were heterogeneous in fasting time, as well as differences in gender, etiology, pharmacological treatment or age, to name a few, could hinder some potential biomarkers. Moreover, plasma metabolites levels could be influenced by many factors such as diet, medications, age and clinical variables (Mauri-Capdevila et al., 2013). However, the use of two cohorts allows overcoming these potential limitations, increasing the robustness of the resulting data (Jove et al., 2015a; Shi et al., 2004). A further limitation of the present work is the fact that many molecules where not identified, although it is a common circumstance for these kind of analyses (Vaniya and Fiehn, 2015). However, the use of orthogonal approaches, such as the use of retention time in standardized chromatographic systems, exact mass and isotope pattern, could help to overcome this limitation, leading to the formulation of potential biomarkers (Sana et al., 2008). Additionally, there is an important step left to be done in order to implement our results in the everyday clinical practice. We have to recognize that metabolomic analysis is too expensive and requires extensive temporal and personal resources. So once potential biomarkers are identified, economic and fast techniques, amenable to most clinical laboratories, need to be developed to detect them. Finally, we included only TIA patients even we knew that the diagnosis of transient ischemia could sometimes be problematic as many conditions mimic this situation. Further research should be done in big tissue-defined ischemia cohorts to confirm our results.

Globally, our data support the existence of metabolic patterns associated with neuroimaging features after transient brain ischemia that could allow the development of serum biomarkers related to acute ischemic lesions and specific acute ischemic patterns.

Supplementary data to this article can be found online at http://dx.doi.org/10.1016/j.ebiom.2016.11.010.

## Funding

This work has been supported by the Government of Catalonia-Agència de Gestió d'Ajuts Universitaris i de Recerca [2009SGR-735 and 2014SGR-1418], the Spanish Ministry of Health [FIS 11-02033, 14-001115 and 14-00328] and the Marató of TV3 Foundation [95/C/2011]. It was also supported by the European Regional Development Fund (PI 14/01115) "A way to build Europe".

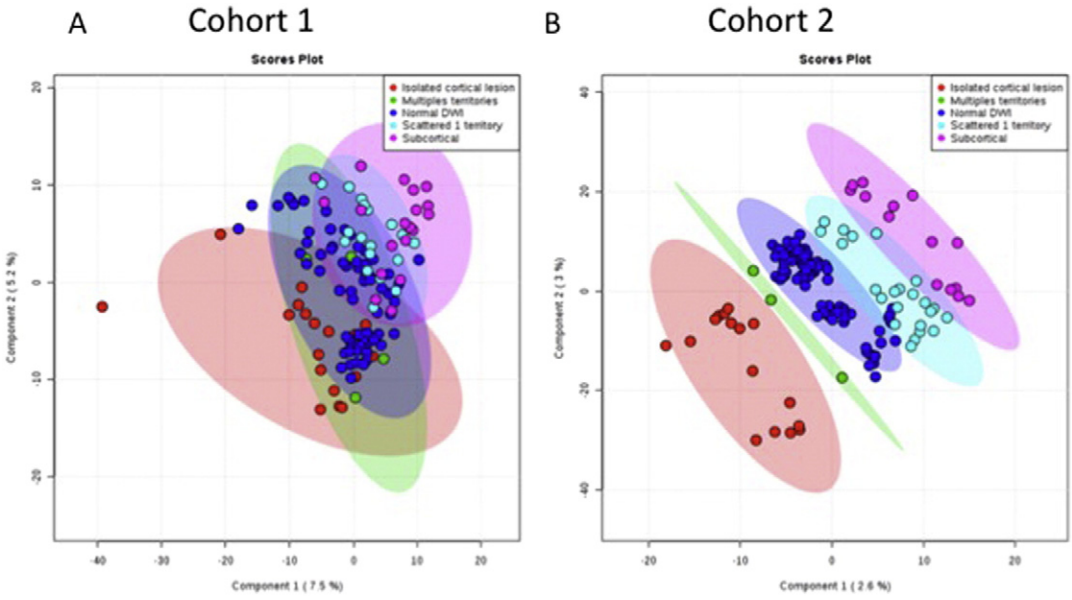


**Fig. 3.** Imaging patterns of ischemia are associated with differential metabolomic profiles. PLSDA model showing association of different ischemia imaging patterns with specific metabolomic profiles, both for the discovery cohort (A) and for the validation cohort (B).

**Table 5**
Molecules differing across DWI patterns.

| Identification[a] | Discovery cohort | | | | Confirmation cohort | | | |
|---|---|---|---|---|---|---|---|---|
| | Mass | RT (min) | p value[b] | Fisher's LSD[c] (n of patients) | Mass | RT (min) | p value[b] | Fisher's LSD[c] (n of patients) |
| LysoPC(16:0)/LysoPE(19:0) | 495.33 | 10.77 | 0.02 | Normal DWI (70)- Isolated cortical lesion (18); **SPOT(18) - Isolated cortical lesion (18)**; Subcortical (19) - Isolated cortical lesion (18) | 495.33 | 10.78 | 0.00 | **Isolated cortical lesion (16) - SPOT (23);** Normal DWI (83) - SPOT (23) |
| 2-Oxo-4-methylthiobutanoic acid | 148.02 | 9.69 | 0.04 | Normal DWI(70) - Isolated cortical lesion (18); Subcortical - Isolated cortical lesion (18) | 148.01 | 9.68 | 0.00 | SPOT (23) - Isolated cortical lesion (16); SPOT (23) - Normal DWI (83) |
| Creatinine | 113.06 | 0.38 | 0.00 | Isolated cortical lesion (18) - Multiples territories (4); Normal DWI(70) - Isolated cortical lesion (18); Subcortical (19) - Isolated cortical lesion (18); Normal DWI(70) - Multiples territories (4); Scattered one territory - Multiples territories (4); Subcortical (19) - Multiples territories (4) | 113.06 | 0.38 | 0.01 | Isolated cortical lesion (16) - SPOT (23); Normal DWI (83) - SPOT (23); Subcortical (14) - SPOT (23) |
| Pyroglutamic acid/N-Acryloylglycine/Pyrroline hydroxycarboxylic acid/4-Oxoproline[d] | 129.04 | 0.65 | 0.02 | **Isolated cortical lesion (18) – SPOT (18)**; **Normal DWI (70)- SPOT(18)**; Subcortical (19) – SPOT (18) | 129.04 | 0.38 | 0.01 | **Isolated cortical lesion (16) - SPOT (23)**; **Normal DWI (83) – SPOT (23)** |
| Unknown1 | 760.03 | 0.34 | 0.05 | **Normal DWI (70)- Isolated cortical lesion (18)**; SPOT (18) - Isolated cortical lesion (18); Subcortical (19) - Isolated cortical lesion (18) | 760.02 | 0.33 | 0.02 | **Normal DWI (83) - Isolated cortical lesion (16)**; Subcortical (14) - Isolated cortical lesion (16); Normal DWI (83) - SPOT (23); Subcortical (14) - SPOT (23) |
| Unknown2 | 825.97 | 0.35 | 0.02 | **SPOT(18) - Normal DWI(70)**; Subcortical (19) - Normal DWI (70) | 825.98 | 0.33 | 0.03 | SPOT (23) - Isolated cortical lesion (16); **SPOT (23) - Normal DWI (83)** |
| Eicosatrienoic acid | 306.26 | 12.17 | 0.05 | Isolated cortical lesion (18)- Normal DWI(70); Isolated cortical lesion (18) - Subcortical (19); **SPOT(18) - Normal DWI(70)**; SPOT (18) – Subcortical (19) | 306.26 | 12.13 | 0.03 | SPOT (23) - Isolated cortical lesion (16); **SPOT (23) - Normal DWI (83)** |

RT, retention time; LysoPC, lysophosphatidylcholine; SPOT, scattered pearls in one arterial territory; DWI, diffusion-weighted images; LysoPE, lysophosphatidylethanolamine.
[a] Potential identities, based on retention time and exact mass are presented. When it is not possible to attribute only one identity, two or three potential identities are shown.
[b] After ANOVA considering different DWI patterns.
[c] Post-hoc analyses using Fisher's Least Significant Difference test, indicating significantly different groups separated by semicolon. Identical differences found in both cohorts are marked by a bold font.
[d] Note the difference in RT between the two cohorts. No peak with similar exact mass and isotope distribution was found closer to the first retention time.

## Author Contributions

Francisco Purroy - Design and conceptualization of the study. Analysis and interpretation of the data. Drafting and revising the manuscript for intellectual content.

Serafí Cambray - Design and conceptualization of the study. Analysis and interpretation of the data. Drafting and revising the manuscript for intellectual content.

Gerard Mauri-Capdevila - Design and conceptualization of the study. Analysis and interpretation of the data. Drafting and revising the manuscript for intellectual content.

Mariona Jové - Design and conceptualization of the study. Analysis and interpretation of the data. Drafting and revising the manuscript for intellectual content.

Jordi Sanahuja - Analysis and interpretation of the data. Revising the manuscript for intellectual content.

Joan Farré - Analysis and interpretation of the data. Revising the manuscript for intellectual content.

Ikram Benabdelhak - Analysis and interpretation of the data. Revising the manuscript for intellectual content.

Jessica Molina-Seguín - Analysis and interpretation of the data. Revising the manuscript for intellectual content.

Laura Colàs-Campàs - Analysis and interpretation of the data. Revising the manuscript for intellectual content.

Robert Begue - Analysis and interpretation of the data. Revising the manuscript for intellectual content.

M. Isabel Gil - Analysis and interpretation of the data. Revising the manuscript for intellectual content.

Reinald Pamplona. Analysis and interpretation of the data. Revising the manuscript for intellectual content and editorial style.

Manuel Portero-Otín - Design and conceptualization of the study. Analysis and interpretation of the data. Drafting and revising the manuscript for intellectual content.

## Acknowledgments

We are indebted to plasma donors for their support and permission. Samples were obtained with the support of IRBLleida biobank and RETICS BIOBANCOS (RD09/0076/00059) and Metabolomics Service from IRBLleida. We would like to thank Rosa Gómez for her technical assistance.

## References

Adams Jr., H.P., Bendixen, B.H., Kappelle, L.J., et al., 1993. Classification of subtype of acute ischemic stroke. Definitions for use in a multicenter clinical trial. TOAST. Trial of Org 10172 in Acute Stroke Treatment. Stroke 24 (1), 35–41.

Amantea, D., Micieli, G., Tassorelli, C., et al., 2015. Rational modulation of the innate immune system for neuroprotection in ischemic stroke. Front. Neurosci. 9, 147.

Anon, 1990. Special report from the National Institute of Neurological Disorders and Stroke. Classification of cerebrovascular diseases III. Stroke 21 (4), 637–676.

Binder, B.Y., Sondergaard, C.S., Nolta, J.A., Leach, J.K., 2013. Lysophosphatidic acid enhances stromal cell-directed angiogenesis. PLoS One 8 (12), e82134.

Bivard, A., Krishnamurthy, V., Stanwell, P., et al., 2014. Spectroscopy of reperfused tissue after stroke reveals heightened metabolism in patients with good clinical outcomes. J. Cereb. Blood Flow Metab. 34 (12), 1944–1950.

Brazzelli, M., Chappell, F., Miranda, H., et al., 2014. Diffusion-weighted imaging and diagnosis of transient ischaemic attack. Ann. Neurol. 75 (1), 67–76.

Easton, J.D., Saver, J.L., Albers, G.W., et al., 2009. Definition and evaluation of transient ischemic attack: a scientific statement for healthcare professionals from the American Heart Association/American Stroke Association Stroke Council; Council on Cardiovascular Surgery and Anesthesia; Council on Cardiovascular Radiology and Intervention; Council on Cardiovascular Nursing; and the Interdisciplinary Council on Peripheral Vascular Disease. The American Academy of Neurology affirms the value of this statement as an educational tool for neurologists. Stroke 40 (6), 2276–2293.

Giles, M.F., Albers, G.W., Amarenco, P., et al., 2011. Early stroke risk and ABCD2 score performance in tissue- vs time-defined TIA: a multicenter study. Neurology 258 (11), 2107–2109.
Halder, S.K., Yano, R., Chun, J., Ueda, H., 2013. Involvement of LPA1 receptor signaling in cerebral ischemia-induced neuropathic pain. Neuroscience 235, 10–15.
Haseruck, N., Erl, W., Pandey, D., et al., 2004. The plaque lipid lysophosphatidic acid stimulates platelet activation and platelet-monocyte aggregate formation in whole blood: involvement of P2Y1 and P2Y12 receptors. Blood 103 (7), 2585–2592.
Jove, M., Portero-Otin, M., Naudi, A., Ferrer, I., Pamplona, R., 2014. Metabolomics of human brain aging and age-related neurodegenerative diseases. J. Neuropathol. Exp. Neurol. 73 (7), 640–657.
Jove, M., Mauri-Capdevila, G., Suarez, I., et al., 2015a. Metabolomics predicts stroke recurrence after transient ischemic attack. Neurology 84 (1), 36–45.
Jove, M., Mauri-Capdevila, G., Suárez, I., et al., 2015b. Metabolomics predicts stroke recurrence after transient ischemic attack. Neurology .
Li, Z.G., Yu, Z.C., Wang, D.Z., et al., 2008. Influence of acetylsalicylate on plasma lysophosphatidic acid level in patients with ischemic cerebral vascular diseases. Neurol. Res. 30 (4), 366–369.
Lista, S., O'Bryant, S.E., Blennow, K., et al., 2015. Biomarkers in sporadic and familial Alzheimer's disease. J. Alzheimers Dis. 47 (2), 291–317.
Liu, X., Hou, J., Shi, L., et al., 2009. Lysophosphatidic acid protects mesenchymal stem cells against ischemia-induced apoptosis in vivo. Stem Cells Dev. 18 (7), 947–954.
Mauri-Capdevila, G., Jove, M., Suarez-Luis, I., Portero-Otin, M., Purroy, F., 2013. Metabolomics in ischaemic stroke, new diagnostic and prognostic biomarkers. Rev. Neurol. 57 (1), 29–36.
McIntyre, R.S., Cha, D.S., Jerrell, J.M., et al., 2014. Advancing biomarker research: utilizing 'Big Data' approaches for the characterization and prevention of bipolar disorder. Bipolar Disord. 16 (5), 531–547.
Merwick, A., Albers, G.W., Amarenco, P., et al., 2010. Addition of brain and carotid imaging to the ABCD(2) score to identify patients at early risk of stroke after transient ischaemic attack: a multicentre observational study. Lancet Neurol. 9 (11), 1060–1069.
Pappa, V., Seydel, K., Gupta, S., et al., 2015. Lipid metabolites of the phospholipase A2 pathway and inflammatory cytokines are associated with brain volume in paediatric cerebral malaria. Malar. J. 14 (1), 513.
Purroy, F., Montaner, J., Rovira, A., Delgado, P., Quintana, M., Alvarez-Sabin, J., 2004. Higher risk of further vascular events among transient ischemic attack patients with diffusion-weighted imaging acute ischemic lesions. Stroke 35 (10), 2313–2319.
Purroy, F., Begue, R., Gil, M.I., et al., 2011. Patterns of diffusion-weighted magnetic resonance imaging associated with etiology improve the accuracy of prognosis after transient ischaemic attack. Eur. J. Neurol. 18 (1), 121–128.
Ren, B., Hale, J., Srikanthan, S., Silverstein, R.L., 2011. Lysophosphatidic acid suppresses endothelial cell CD36 expression and promotes angiogenesis via a PKD-1-dependent signaling pathway. Blood 117 (22), 6036–6045.
Ren, Z., Yang, N., Ji, C., et al., 2015. Neuroprotective effects of 5-(4-hydroxy-3-dimethoxybenzylidene)-thiazolidinone in MPTP induced Parkinsonism model in mice. Neuropharmacology 93, 209–218.
Rosset, A., Spadola, L., Ratib, O., 2004. OsiriX: an open-source software for navigating in multidimensional DICOM images. J. Digit. Imaging 17 (3), 205–216.
Sana, T.R., Roark, J.C., Li, X., Waddell, K., Fischer, S.M., 2008. Molecular formula and METLIN Personal Metabolite Database matching applied to the identification of compounds generated by LC/TOF-MS. J. Biomol. Tech. 19 (4), 258–266.
Shi, H., Paolucci, U., Vigneau-Callahan, K.E., Milbury, P.E., Matson, W.R., Kristal, B.S., 2004. Development of biomarkers based on diet-dependent metabolic serotypes: practical issues in development of expert system-based classification models in metabolomic studies. OMICS 8 (3), 197–208.
Srikrishna, G., Toomre, D.K., Manzi, A., et al., 2001. A novel anionic modification of N-glycans on mammalian endothelial cells is recognized by activated neutrophils and modulates acute inflammatory responses. J. Immunol. 166 (1), 624–632.
Vaniya, A., Fiehn, O., 2015. Using fragmentation trees and mass spectral trees for identifying unknown compounds in metabolomics. Trends Anal. Chem. 69, 52–61.
Vingara, L.K., Yu, H.J., Wagshul, M.E., et al., 2013. Metabolomic approach to human brain spectroscopy identifies associations between clinical features and the frontal lobe metabolome in multiple sclerosis. NeuroImage 82, 586–594.
Waddington, J.L., 2007. Neuroimaging and other neurobiological indices in schizophrenia: relationship to measurement of functional outcome. Br. J. Psychiatry Suppl. 50, s52–s57.
Wikoff, W.R., Pendyala, G., Siuzdak, G., Fox, H.S., 2008. Metabolomic analysis of the cerebrospinal fluid reveals changes in phospholipase expression in the CNS of SIV-infected macaques. J. Clin. Invest. 118 (7), 2661–2669.